

Coupling/decoupling between translational and rotational dynamics in a supercooled molecular liquid

Song-Ho Chong¹ and Walter Kob²

¹*Institute for Molecular Science, Okazaki 444-8585, Japan*

²*Laboratoire des Colloïdes, Verres et Nanomatériaux,
UMR 5587 CNRS, Université Montpellier 2, 34095 Montpellier, France*

(Dated: December 11, 2008)

We use molecular dynamics computer simulations to investigate the coupling/decoupling between translational and rotational dynamics in a glass-forming liquid of dumbbells. This is done via a careful analysis of the α -relaxation time τ_q^C of the incoherent center-of-mass density correlator at the structure factor peak, the α -relaxation time τ_2 of the reorientational correlator, and the translational (D_t) and rotational (D_r) diffusion constants. We find that the coupling between the relaxation times τ_q^C and τ_2 increases with decreasing temperature T , whereas the coupling decreases between the diffusivities D_t and D_r . In addition, the T -dependence of D_t decouples from that of $1/\tau_2$, which is consistent with previous experiments and has been interpreted as a signature of the “translation-rotation decoupling.” We trace back these apparently contradicting observations to the dynamical heterogeneities in the system. We show that the decreasing coupling in the diffusivities D_t and D_r is only apparent due to the inadequacy of the concept of the rotational diffusion constant for describing the reorientational dynamics in the supercooled state. We also argue that the coupling between τ_q^C and τ_2 and the decoupling between D_t and $1/\tau_2$, both of which strengthen upon cooling, can be consistently understood in terms of the growing dynamic length scale.

PACS numbers: 64.70.pm, 61.20.Ja, 61.20.Lc, 61.25.Em

One of the puzzling features of glass-forming systems is that upon cooling the translational dynamics appears to decouple from the rotational dynamics [1, 2, 3, 4, 5]. At high temperatures, the translational and rotational diffusion coefficients, D_t and D_r , respectively, are inversely proportional to η/T , where η is the viscosity and T the temperature, in agreement with the Stokes-Einstein (SE) and the Stokes-Einstein-Debye (SED) relation. Below approximately $1.2T_g$, with T_g the glass transition temperature, the SE relation is replaced by a fractional relation $D_t \propto (\eta/T)^{-\xi}$ with $\xi < 1$, implying a more enhanced translational diffusion than predicted by the viscosity, whereas D_r remains proportional to $(\eta/T)^{-1}$ down to T_g [1, 2]. On the other hand, recent computer simulations give evidence for a stronger correlation between translational and rotational mobilities at lower T [6, 7], which is apparently in contradiction with the mentioned decoupling between D_t and D_r . In addition, an enhancement of rotational diffusion relative to translation upon cooling is reported in these simulations, which is a trend opposite to that observed in experiments [1, 2]. In this Letter, we report computer simulation results for gaining more insight and unified understanding of these coupling/decoupling phenomena in the supercooled state.

The system we consider is the binary mixture of rigid, symmetric dumbbell molecules, denoted as AA and BB dumbbells, studied in Ref. [8]. Each molecule consists of two identical fused Lennard-Jones (LJ) particles of type A or B having the same mass m , and their bond lengths are denoted by l_{AA} and l_{BB} . The interaction between two molecules is given by the sum of the LJ interactions $V_{\alpha\beta}(r)$ between the four constituent sites, with the LJ

parameters $\epsilon_{\alpha\beta}$ and $\sigma_{\alpha\beta}$ for $\alpha, \beta \in \{A, B\}$ taken from Ref. [9], which are slightly modified so that $V_{\alpha\beta}(r)$ and $V'_{\alpha\beta}(r)$ are zero at the cutoff $r_{\text{cut}} = 2.5\sigma_{\alpha\beta}$ (see Ref. [8] for details). Bond lengths are specified by a parameter $\zeta \equiv l_{AA}/\sigma_{AA} = l_{BB}/\sigma_{BB}$, and a sufficiently large value $\zeta = 0.8$ is chosen so that anomalous reorientational dynamics caused by the so-called type-A transition is absent [8, 10]. The number of AA and BB dumbbells is $N_{AA} = 800$ and $N_{BB} = 200$. In the following all quantities are expressed in reduced units with the unit of length σ_{AA} , the unit of energy ϵ_{AA} (setting $k_B = 1$), and the unit of time $(m\sigma_{AA}^2/\epsilon_{AA})^{1/2}$. Standard molecular dynamics simulations have been performed as in Ref. [9] with the cubic box of length $L = 10.564$ for $2.0 \leq T \leq 10$. The longest runs were 2×10^9 time steps, and we performed 16 independent runs to improve the statistics. Such long simulations were necessary to reach below the critical temperature T_c of the mode-coupling theory [11], which we estimate as $T_c \approx 2.10$ based on an analysis similar to the one done in Ref. [9]. In experiments T_c is found to be $\approx 1.2T_g$ [12], i.e., close to the temperature at which the aforementioned decoupling sets in [1]. We also introduce the onset temperature, found to be $T_{\text{onset}} \approx 4.0$, below which correlators exhibit the two-step relaxation, a characteristic feature of the glassy dynamics in which molecules are temporarily caged by their neighbors. Hereafter, all quantities used in our discussion refer to those for AA dumbbells, and the subscript AA shall be dropped for notational simplicity.

In the present study we will characterize the translational dynamics by the incoherent center-of-mass density correlator $F_q^C(t) = (1/N) \sum_j \langle e^{i\vec{q} \cdot [\vec{r}_j^C(t) - \vec{r}_j^C(0)]} \rangle$, and

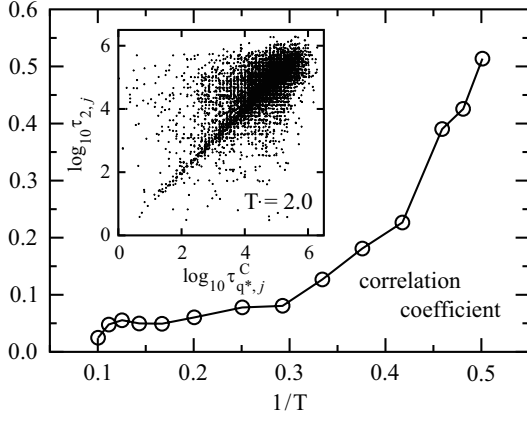


FIG. 1: Correlation coefficient between $\tau_{q^*,j}^C$ and $\tau_{2,j}$ as a function of $1/T$. The Inset is a scatter plot of $\tau_{2,j}$ versus $\tau_{q^*,j}^C$ for $T = 2.0$ on double logarithmic scales.

the rotational dynamics by $C_\ell(t) = (1/N) \sum_j \langle P_\ell[\vec{e}_j(t) \cdot \vec{e}_j(0)] \rangle$. Here $\vec{r}_j^C(t)$ and $\vec{e}_j(t)$ denote the center-of-mass position and the orientation of the j th molecule at time t , respectively, and P_ℓ is the Legendre polynomial of order ℓ . The α -relaxation times τ_q^C and τ_ℓ shall be defined via $F_q^C(\tau_q^C) = 0.1$ and $C_\ell(\tau_\ell) = 0.1$.

Previous simulation studies have used various ways to classify particle mobility [6, 7, 13, 14, 15]. In this Letter, translational and rotational mobilities of individual molecule shall be classified in terms of the *first passage times*, $\tau_{q,j}^C$ and $\tau_{\ell,j}$, at which individual-molecule quantities $e^{i\vec{q} \cdot [\vec{r}_j^C(t) - \vec{r}_j^C(0)]}$ (averaged over \vec{q} having the same modulus q) and $P_\ell[\vec{e}_j(t) \cdot \vec{e}_j(0)]$ become zero for the first time. We confirmed that $\tau_q^C \propto (1/N) \sum_j \tau_{q,j}^C$ and $\tau_\ell \propto (1/N) \sum_j \tau_{\ell,j}$ hold, and hence, $\tau_{q,j}^C$ and $\tau_{\ell,j}$ can also be regarded as individual molecule's relaxation times. In the following, we will mainly refer to the structure factor peak position $q^* = 8.0$ and $\ell = 2$ because of their experimental significance [1, 2, 16].

The Inset of Fig. 1 shows a scatter plot of $\tau_{2,j}$ versus $\tau_{q^*,j}^C$ for $T = 2.0$. We recognize that there is a strong correlation between these two quantities, in particular for the molecules that move/rotate quickly. From such a scatter plot we can calculate the correlation coefficient and its T -dependence is shown in the main panel of Fig. 1. We see that the correlation between translation and rotation increases quickly with decreasing T , showing the strong coupling between these two types of motions at low temperatures, in agreement with the findings in recent simulation studies [6, 7].

We also mention that the molecules that have a high translational mobility are clustered in space, in agreement with the findings for other glass formers [7, 14, 15], and the same is true for those rotating quickly. This result is in accord with the correlation shown in Fig. 1.

We next consider the translational (D_t) and rotational

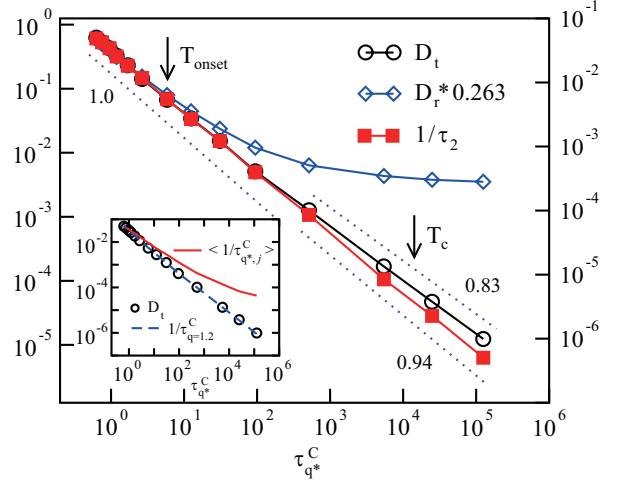


FIG. 2: (Color online) Log-log plot of the translational diffusion coefficient D_t (circles, right scale), the rotational diffusion coefficient D_r (diamonds, right scale, shifted so that D_t and D_r agree at high T), and the inverse of the rotational relaxation time $1/\tau_2$ (filled squares, left scale) versus the α -relaxation time $\tau_{q^*}^C$. The dotted straight lines refer to $(\tau_{q^*}^C)^{-x}$ with the exponents x cited in the figure. The arrows indicate the locations of T_{onset} and T_c . Inset: D_t (circles) from the main panel is compared with $\langle 1/\tau_{q^*,j}^C \rangle$ (solid line) and $1/\tau_q^C$ for $q = 1.2$ (dashed line), which are vertically shifted so that they agree with D_t at high T .

(D_r) diffusion coefficients. D_t is determined via $D_t = \lim_{t \rightarrow \infty} \Delta r_C^2(t)/6t$ of the center-of-mass mean-squared displacement $\Delta r_C^2(t) = (1/N) \sum_j \langle [\vec{r}_j^C(t) - \vec{r}_j^C(0)]^2 \rangle$. D_r is calculated using the Einstein formulation [17], i.e., via $D_r = \lim_{t \rightarrow \infty} \Delta \phi^2(t)/4t$ of the mean-squared angular displacement

$$\Delta \phi^2(t) = (1/N) \sum_j \sum_{\alpha=X,Y} \langle \Delta \phi_{j,\alpha}(t)^2 \rangle. \quad (1)$$

Here $\Delta \phi_{j,\alpha}(t) = \int_0^t dt' \omega_{j,\alpha}(t')$ with $\omega_{j,\alpha}(t)$ denoting the α -component of the angular velocity of the j th molecule. Note that for linear molecules, the summation over α is for the two directions X and Y perpendicular to the Z axis chosen along $\vec{e}_j(0)$ [18].

Figure 2 shows the log-log plot of D_t (circles) and D_r (diamonds) versus $\tau_{q^*}^C$. Thus, this graph mimics Fig. 5 of Ref. [1] where D_t and D_r for orthoterphenyl are traced as a function of η/T . We have used $\tau_{q^*}^C$ as a substitute for η/T since accurate calculation of η is computationally challenging. However, this approximation should be quite accurate since the α -relaxation time at the structure factor peak position is known to track η/T [16].

From Fig. 2 we see that $D_t \propto (\tau_{q^*}^C)^{-1}$ holds at high T , whereas it is replaced by a fractional relation $D_t \propto (\tau_{q^*}^C)^{-0.83}$ for $T \lesssim T_c$. This anomalous behavior (the breakdown of the SE relation) and its occurrence near $T_c \approx 1.2 T_g$ are in agreement with experiments [1]. For D_r we recognize that $D_r \propto (\tau_{q^*}^C)^{-1}$, and hence $D_r \propto D_t$,

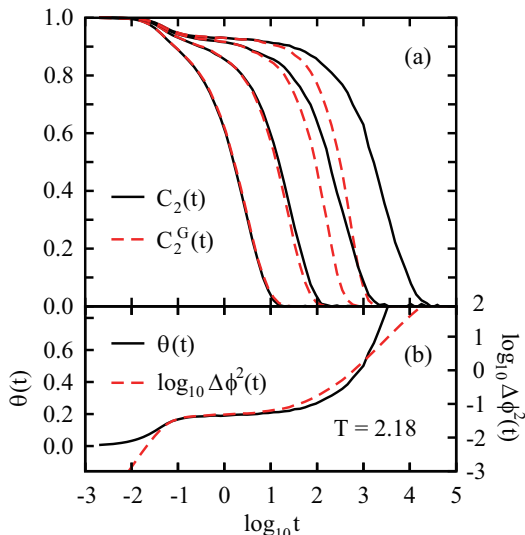


FIG. 3: (Color online) (a) The reorientational correlator $C_2(t)$ (solid lines) and the one calculated within the Gaussian approximation $C_2^G(t)$ (dashed lines) versus $\log_{10} t$ for $T = 5.0, 3.0, 2.39$, and 2.18 (from left to right). (b) The average orientation $\theta(t)$ (left scale) and the logarithm of the mean-squared angular displacement $\log_{10} \Delta\phi^2(t)$ (right scale) for $T = 2.18$.

hold at high T , but that this quantity strongly decouples from D_t for $T < T_{\text{onset}}$. That the T -dependence of D_r is weaker than the one of D_t is in contradiction to the trend observed in experiments [1], but is in agreement with other recent simulation studies [6, 7].

Let us notice that the experiment in Ref. [1] does not directly probe D_r , but determines D_r from the measurement of τ_2 via the relation $D_r \propto 1/\tau_2$ predicted by the Debye model. Thus, what is reported as D_r in Ref. [1] corresponds in fact to $1/\tau_2$. In Fig. 2 we have also included our simulation results for $1/\tau_2$ and we see that τ_2 correlates well with $\tau_{q^*}^C$, in accord with our previous discussion for the relaxation times, although a slight deviation from the strict proportionality is discernible for $T \lesssim T_c$. Thus, by identifying $\tau_{q^*}^C$ with η/T , our simulation result for $1/\tau_2$ is in accord with the experiment [1] in which one finds $1/\tau_2 \propto (\eta/T)^{-1}$ down to T_g . Therefore, the decoupling of D_r from $1/\tau_2$ shown in Fig. 2 only indicates that the Debye model breaks down for $T < T_{\text{onset}}$, and hence, $1/\tau_2$ should not be considered as being proportional to D_r in the supercooled state.

To understand why D_t and D_r behave so differently, we analyze the breakdown of the Debye model in more detail. Within the Gaussian approximation one has $C_\ell^G(t) = \exp[-\ell(\ell+1)\Delta\phi^2(t)/4]$ [18]. The long-time behavior is given by $C_\ell^G(t) = \exp[-\ell(\ell+1)D_r t]$, which agrees with the prediction from the Debye model. From Fig. 2 one therefore expects that the Gaussian approximation breaks down for $T < T_{\text{onset}} \approx 4.0$, and this is indeed the case as shown in Fig. 3a.

Figure 3a also implies that for $T < T_{\text{onset}}$ there ex-

ists a time window during which $\Delta\phi^2(t)$ increases significantly although the orientation of a molecule hardly changes. The existence of such a window is demonstrated in Fig. 3b for a representative temperature, from which one recognizes that $\Delta\phi^2(t)$ starts to increase noticeably at $\log_{10} t \approx 1$ whereas the average orientation $\theta(t) = (1/N) \sum_j \langle \cos^{-1}[\vec{e}_j(t) \cdot \vec{e}_j(0)] \rangle$ remains nearly constant up to $\log_{10} t \approx 2$.

The appearance of the plateau in $C_2(t)$ and $\theta(t)$ for $T < T_{\text{onset}}$ reflects the librational motion of a molecule trapped inside the cage, with the orientation $\vec{e}_j(t)$ of the molecule remaining close to $\vec{e}_j(0)$. (For the translational degrees of freedom this corresponds to rattling of the center-of-mass position.) If the average orientation during the librational motion coincides with $\vec{e}_j(0)$, this gives rise to a diffusive movement of $\Delta\phi_{j,z}(t)$ [17], which however does not contribute to $\Delta\phi^2(t)$, see Eq. (1). If, on the other hand, the average orientation is tilted from $\vec{e}_j(0)$, one can show that $\Delta\phi_{j,x}(t)$ and $\Delta\phi_{j,y}(t)$ also exhibit a diffusive movement. Thus, a diffusive increase in $\Delta\phi^2(t)$ occurs even if the molecule has not yet reoriented and is still performing the librational motion inside the cage, and this effect explains the difference between $\log_{10} \Delta\phi^2(t)$ and $\theta(t)$ at intermediate times as seen in Fig. 3b. D_r from the Einstein formulation is thus more affected by the librational motion than the real “reorientational” dynamics, leading to a spurious “decoupling” between D_t and D_r . Since there is no other proper way to define D_r , we conclude that the concept of the rotational diffusion constant is inadequate for describing the reorientational dynamics in the supercooled state.

Now let us turn our attention to the decoupling between $1/\tau_{q^*}^C$ and D_t , and between $1/\tau_2$ and D_t , which occurs near and below T_c (see Fig. 2). The latter is known as the “translation-rotation decoupling.” It was conjectured that such a decoupling arises because $1/\tau_2$ and D_t reflect different moments of the distribution of relaxation times, i.e., $1/\tau_2 \propto 1/\langle \tau_{2,j} \rangle$ while $D_t \propto \langle 1/\tau_{q^*,j}^C \rangle$ [4]. The essential ingredient of this conjecture is the assumption that local translational mobility is proportional to local rotational mobility [4], which is justified from our simulation (see Fig. 1). However, while $\tau_2 \propto \langle \tau_{2,j} \rangle$ has been confirmed from our simulation, the T -dependence of $\langle 1/\tau_{q^*,j}^C \rangle$ is not in accord with that of D_t as demonstrated in the Inset of Fig. 2. On the other hand, as also shown there, the inverse of the α -relaxation time $1/\tau_q^C$ for $q = 1.2$ is found to track D_t in the simulated T range.

That $D_t \propto (\tau_{q=1.2}^C)^{-1}$ while $D_t \propto (\tau_{q^*}^C)^{-0.83}$ for $T \lesssim T_c$ can be understood in terms of the growing onset length scale l_{onset} of Fickian diffusion [19, 20]. Here, l_{onset} is defined so that the relaxation time τ_q^C for $2\pi/q < l_{\text{onset}}$ decouples from the diffusivity D_t , and can be estimated from the ratio R_q^C of the product $q^2 D_t \tau_q^C$ to the one at some reference temperature T_{ref} with a procedure detailed in Ref. [20]. (In the present work we have chosen $T_{\text{ref}} = 5.0$ and a criterion $R_q^C = 1.2$ for determin-

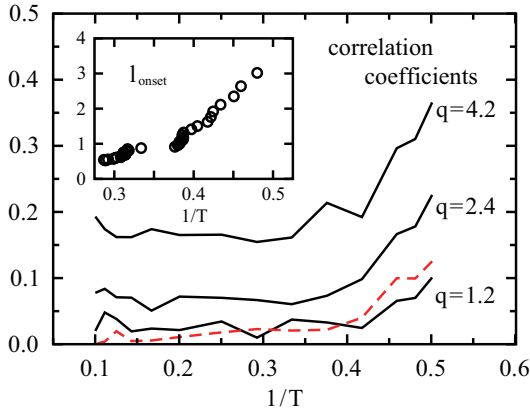


FIG. 4: (Color online) Correlation coefficients between $\tau_{q,j}^C$ and $\tau_{q,j}^C$'s (solid lines) for $q = 4.2, 2.4$, and 1.2 versus $1/T$. The dashed line denotes the correlation coefficient between $\tau_{2,j}$ and $\tau_{q=1.2,j}^C$. The Inset exhibits the length scale l_{onset} introduced in the text as a function of $1/T$.

ing l_{onset} .) The resulting l_{onset} as a function of $1/T$ is presented in the Inset of Fig. 4, from which one finds $l_{\text{onset}} \approx 3$ for $1/T \approx 1/T_c = 0.48$. Thus, $D_t \propto (\tau_{q=1.2}^C)^{-1}$ for $T \lesssim T_c$ since the associated length scale $2\pi/1.2 \approx 5.2$ exceeds l_{onset} , whereas $\tau_{q^*}^C$ decouples from D_t since $2\pi/q^* \approx 0.8$ is smaller than l_{onset} .

To what extent the dynamics occurring on different length scales are correlated is examined in the main panel of Fig. 4, where correlation coefficients between $\tau_{q,j}^C$ and $\tau_{q,j}^C$'s for $q = 4.2, 2.4$, and 1.2 are plotted with solid lines. The mentioned decoupling between $\tau_{q^*}^C$ and $\tau_{q=1.2}^C$ is reflected in the small value ($\lesssim 0.1$) of the corresponding correlation coefficient. On the other hand, one infers from Fig. 4 that a significant correlation, characterized, e.g., by the correlation coefficient exceeding 0.2, develops between $\tau_{q,j}^C$ and $\tau_{q=4.2,j}^C$ for $1/T \gtrsim 0.4$, where l_{onset} becomes larger than the associated length scale $2\pi/4.2 \approx 1.5$. Similarly, one finds that the correlation coefficient between $\tau_{q,j}^C$ and $\tau_{q=2.4,j}^C$ exceeds 0.2 only for $1/T \gtrsim 0.5$, where l_{onset} is larger than $2\pi/2.4 \approx 2.6$. Thus, though originally introduced as the onset length scale of Fickian diffusion, l_{onset} also provides a coherent length in the sense that the dynamics occurring on length scales smaller than l_{onset} develop significant correlations.

Let us estimate the length scale associated with τ_2 utilizing such a “coherent length” l_{onset} . One finds from Fig. 1 that the correlation coefficient between $\tau_{q,j}^C$ and $\tau_{2,j}$ exceeds 0.2 for $1/T \gtrsim 0.4$. According to the mentioned interpretation of l_{onset} , the dynamics responsible for $\tau_{q^*}^C$ and τ_2 become correlated if both of their characteristic length scales become smaller than l_{onset} . Thus, the length scale associated with τ_2 can be estimated as ≈ 1.5 which is determined by l_{onset} at $1/T \approx 0.4$ (see Fig. 4). This explains why the correlation coefficient between $\tau_{2,j}$ and $\tau_{q=1.2,j}^C$ is small ($\lesssim 0.1$) as shown with

the dashed line in Fig. 4, i.e., why $1/\tau_2$ decouples from $(\tau_{q=1.2}^C)^{-1} \propto D_t$.

Thus, the translation-rotation decoupling between D_t and τ_2 should more properly be understood as the decoupling of the dynamics occurring on different length scales, which arises due to the growing dynamic length scale. This notion also explains the decoupling between $\tau_{q^*}^C$ and D_t (the breakdown of the SE relation), as well as the translation-rotation “coupling” between $\tau_{q^*}^C$ and τ_2 occurring on comparable length scales.

We thank W. Götze for discussions. This work has been supported by Grant-in-Aids for scientific research from the Ministry of Education, Culture, Sports, Science and Technology of Japan (No. 20740245).

-
- [1] F. Fujara, B. Geil, H. Sillescu, and G. Fleischer, *Z. Phys. B* **88**, 195 (1992).
 - [2] M. T. Cicerone and M. D. Ediger, *J. Chem. Phys.* **104**, 7210 (1996).
 - [3] L. Andreozzi, A. Di Schino, M. Giordano, and D. Leporini, *Europhys. Lett.* **38**, 669 (1997).
 - [4] M. D. Ediger, *Annu. Rev. Phys. Chem.* **51**, 99 (2000).
 - [5] P. G. Debenedetti and F. H. Stillinger, *Science* **410**, 259 (2001).
 - [6] M. G. Mazza, N. Giovambattista, F. W. Starr, and H. E. Stanley, *Phys. Rev. Lett.* **96**, 057803 (2006); M. G. Mazza, N. Giovambattista, H. E. Stanley, and F. W. Starr, *Phys. Rev. E* **76**, 031203 (2007).
 - [7] T. G. Lombardo, P. G. Debenedetti, and F. H. Stillinger, *J. Chem. Phys.* **125**, 174507 (2006).
 - [8] S.-H. Chong, A. J. Moreno, F. Sciortino, and W. Kob, *Phys. Rev. Lett.* **94**, 215701 (2005).
 - [9] W. Kob and H. C. Andersen, *Phys. Rev. Lett.* **73**, 1376 (1994).
 - [10] S.-H. Chong and W. Götze, *Phys. Rev. E* **65**, 041503 (2002); S.-H. Chong and W. Götze, *Phys. Rev. E* **65**, 051201 (2002).
 - [11] W. Götze and L. Sjögren, *Rep. Prog. Phys.* **55**, 241 (1992).
 - [12] E. Rössler, *Ber. Bunsenges. Phys. Chem.* **94**, 392 (1990).
 - [13] J. Qian, R. Hentschke, and A. Heuer, *J. Chem. Phys.* **110**, 4514 (1999).
 - [14] L. Berthier, *Phys. Rev. E* **69**, 020201(R) (2004).
 - [15] G. A. Appignanesi, J. A. Rodriguez Fris, R. A. Montani, and W. Kob, *Phys. Rev. Lett.* **96**, 057801 (2006).
 - [16] F. Mezei, W. Knaak, and B. Farago, *Phys. Rev. Lett.* **58**, 571 (1987); R. Yamamoto and A. Onuki, *Phys. Rev. Lett.* **81**, 4915 (1998).
 - [17] S. Kämmerer, W. Kob, and R. Schilling, *Phys. Rev. E* **56**, 5450 (1997).
 - [18] R. M. Lynden-Bell, in *Molecular Liquids*, edited by A. J. Barnes, W. J. Orville-Thomas, and J. Yarwood (Reidel, Dordrecht, 1984), p. 501; R. M. Lynden-Bell and W. A. Steele, *J. Phys. Chem.* **88**, 6514 (1984).
 - [19] L. Berthier, D. Chandler, and J. P. Garrahan, *Europhys. Lett.* **69**, 320 (2005).
 - [20] S.-H. Chong, *Phys. Rev. E* **78**, 041501 (2008).